INFECTION AND IMMUNITY, Nov. 2001, p. 7106–7120 Vol. 69, No. 11
0019-9567/01/$04.00+0 DOI: 10.1128/IAI.69.11.7106–7120.2001

Three-Dimensional Tissue Assemblies: Novel Models for the Study of *Salmonella enterica* Serovar Typhimurium Pathogenesis

CHERYL A. NICKERSON,[1]* THOMAS J. GOODWIN,[2] JACQUELINE TERLONGE,[1] C. MARK OTT,[3] KENT L. BUCHANAN,[1] WILLIAM C. UICKER,[1] KAMAL EMAMI,[3] CARLY L. LEBLANC,[1] RAJEE RAMAMURTHY,[1] MARK S. CLARKE,[4] CHARLES R. VANDERBURG,[5] TIMOTHY HAMMOND,[6] AND DUANE L. PIERSON[2]

Program in Molecular Pathogenesis and Immunity, Department of Microbiology and Immunology, Tulane University School of Medicine, New Orleans, Louisiana 70112[1]; Life Sciences Research Laboratories, NASA-Johnson Space Center,[2] EASI/Wyle Laboratories, Johnson Space Center,[3] and Universities Space Research Association, Division of Space Life Sciences,[4] Houston, Texas 77058; Massachusetts General Hospital, Boston, Massachusetts 02114[5]; and Section of Nephrology, Tulane University Medical Center, New Orleans, Louisiana 70112-2699[6]

Received 13 June 2001/Returned for modification 23 July 2001/Accepted 15 August 2001

The lack of readily available experimental systems has limited knowledge pertaining to the development of *Salmonella*-induced gastroenteritis and diarrheal disease in humans. We used a novel low-shear stress cell culture system developed at the National Aeronautics and Space Administration in conjunction with cultivation of three-dimensional (3-D) aggregates of human intestinal tissue to study the infectivity of *Salmonella enterica* serovar Typhimurium for human intestinal epithelium. Immunohistochemical characterization and microscopic analysis of 3-D aggregates of the human intestinal epithelial cell line Int-407 revealed that the 3-D cells more accurately modeled human in vivo differentiated tissues than did conventional monolayer cultures of the same cells. Results from infectivity studies showed that *Salmonella* established infection of the 3-D cells in a much different manner than that observed for monolayers. Following the same time course of infection with *Salmonella*, 3-D Int-407 cells displayed minimal loss of structural integrity compared to that of Int-407 monolayers. Furthermore, *Salmonella* exhibited significantly lower abilities to adhere to, invade, and induce apoptosis of 3-D Int-407 cells than it did for infected Int-407 monolayers. Analysis of cytokine expression profiles of 3-D Int-407 cells and monolayers following infection with *Salmonella* revealed significant differences in expression of interleukin 1α (IL-1α), IL-1β, IL-6, IL-1Ra, and tumor necrosis factor alpha mRNAs between the two cultures. In addition, uninfected 3-D Int-407 cells constitutively expressed higher levels of transforming growth factor β1 mRNA and prostaglandin E_2 than did uninfected Int-407 monolayers. By more accurately modeling many aspects of human in vivo tissues, the 3-D intestinal cell model generated in this study offers a novel approach for studying microbial infectivity from the perspective of the host-pathogen interaction.

While important advances have been made toward understanding how *Salmonella* interacts with the intestinal epithelium to initiate disease (reviewed in references 6 and 44), investigations into the interaction of *Salmonella* with the human intestinal epithelium have been limited by the lack of in vitro and in vivo models which faithfully replicate the in vivo condition. In particular, it is well documented that important differences exist between the pathogenesis of *Salmonella enterica* serovar Typhimurium in human infections and that in widely used cell culture and animal models (34, 40, 47). In vitro assays using cultured mammalian epithelial cells have long been used as a model for investigating the interaction between *Salmonella* and the intestinal mucosa. However, there are inherent limitations associated with the use of these cultured cell lines (34), as they are not exact models of the conditions faced in vivo by *Salmonella*. Several characteristics of conventional tissue culture models have raised concerns regarding their overall efficacy as models for microbial infectivity in general (34) due to the dedifferentiation of these cells during conventional cell culture. Indeed, many of the physiological differences between cultured cells and their in vivo counterparts are believed to be the result of the dissociation of cells from their native three-dimensional (3-D) geometry in vivo to their propagation on a two-dimensional substrate in vitro (10). Likewise, many characteristics of animal models fail to mimic the human disease, and animal models present a complex system in which many variables cannot be controlled. A high-fidelity enteric cell culture model could provide new insights into studies of *Salmonella* infectivity by bridging the gap between the inherent limitations of cultured mammalian cells and intact animals.

For humans, *S. enterica* serovar Typhimurium is among the most common *Salmonella* serotypes isolated from individuals suffering from infectious gastroenteritis and has long been recognized as a major public health problem (23). Gastroenteritis results from infection of the small intestine after ingestion with *Salmonella*. Indeed, the ability to colonize the intestinal epithelium is an essential feature in the pathogenicity of *Salmonella* infection. Moreover, the initial interactions between *Salmonella* and the host intestinal epithelium are believed to play a key role in mediating the intense inflammatory and secretory response which is a hallmark of serovar Typhimurium infections in humans (reviewed in reference 6). Studies with cultured intestinal epithelial cells have shown that,

* Corresponding author. Mailing address: Program in Molecular Pathogenesis and Immunity, Department of Microbiology and Immunology, SL38, Tulane University Medical School, 1430 Tulane Ave., New Orleans, LA 70112. Phone: (504) 988-4609. Fax: (504) 588-5144. E-mail: cnicker@tulane.edu.

FIG. 1. Operation of the RWV. The cylindrical culture vessel is filled with culture medium, and the cells or tissue particles are added. All air bubbles are removed from the culture vessel. The vessel is attached to the rotator base and rotated about the horizontal axis (power supply not shown). Cell aggregate particles establish a fluid orbit within the culture medium in the rotating vessel. They do not collide with the walls or any other parts of the vessel. As 3-D tissues grow in size, the rotation speed is adjusted to compensate for the increased settling rates of the larger particles. The tissue particles do move enough within the fluid culture medium to exchange nutrients, wastes, and dissolved gases and make contact with other tissue particles. The cells and/or tissue particles join to form larger tissue particles that continue the differentiation process. Oxygen supply and carbon dioxide removal are achieved through a gas-permeable silicone rubber membrane.

shortly after contact, *Salmonella* engages host cells in a complex biochemical cross talk, which triggers host-cell signal transduction pathways ultimately resulting in host cytoskeleton rearrangement, cell membrane ruffling, bacterial uptake, and production of prostaglandins and proinflammatory cytokines (reviewed in reference 6).

In the present study, we present a novel use of an innovative form of optimized suspension culture, the rotating-wall vessel (RWV), to examine the infectivity of serovar Typhimurium for human intestinal epithelium. The RWV (Fig. 1) is an optimized form of suspension culture that due to its low-shear and low-turbulence operation minimizes mechanical cell damage and allows cells to associate into 3-D structures, thereby promoting cellular differentiation (reviewed in references 21 and 41). Accordingly, the RWV largely solves the challenges of suspension culture: to suspend cells and microcarriers without inducing turbulence, or high degrees of shear, while providing adequate nutrition and oxygenation. In this environment, dissociated cells can assemble into high-fidelity 3-D tissue aggregates, several millimeters in size, which are largely devoid of necrotic cores (reviewed in references 21 and 41).

The primary advantage of the RWV over either dynamic or static tissue culture systems is that its low-shear environment allows cells to aggregate, grow three-dimensionally, and differentiate. This advantage results in cells or tissues that very closely resemble the in vivo tissue equivalent (reviewed in references 21 and 41). In conventional static flat-culture flasks or dishes, the two-dimensional environment and plastic substrate tend to alter gene expression and prevent differentiation (10, 21). Because the cells are maintained in a gentle fluid orbit, cells grown in the RWV are able to attach to one another, form complex 3-D structures, and attain a more tissue-like phenotype. Thus, unlike cell and tissue cultures grown in two-dimensional flat-plate systems, cells cultured in the RWV are functionally similar to tissues in the human body (reviewed in references 21 and 41). Accordingly, the RWV bioreactors offer a novel approach not previously applied for studying microbial infectivity from the perspective of the host-pathogen interaction.

We used the RWV bioreactors in conjunction with cultivation of 3-D aggregates of the human embryonic small intestinal epithelial cell line Int-407 (ATCC CCL-6), to study the infectivity of serovar Typhimurium for human intestinal epithelium. While the Int-407 cell line contains a mix of human small intestinal epithelial cells and HeLa cells (cervical adenocarcinoma), we chose it as the model system for this study for several important reasons. First, the Int-407 cell line is isolated from normal human small intestine, which is the initiating site of infection for *Salmonella* species. Second, Int-407 cells have been, historically, one of the most extensively used cell lines for the study of the interactions occurring between *Salmonella* and the host intestinal epithelium. Indeed, several landmark studies which characterized the early stages of *Salmonella* infection, including adherence and invasion, elicitation of cytokine and chemokine responses, and signal transduction, have used the Int-407 cell line (5, 37, 39, 45). Third, when grown as conventional monolayers, Int-407 cells are poorly differentiated, lack polarity, do not produce mucus, and lack many other physiological features associated with their in vivo counterparts, including tight junctions, desmosomes, and secretory granules. Thus, the ability of Int-407 cells to differentiate during culture in the RWV bioreactor could be readily measured. Fourth, Int-407 cells were isolated from embryonic tissues and were immortalized before they completed their differentiation process—thus, they have the potential to manifest numerous characteristics of in vivo tissues. Accordingly, the Int-407 cell line provided us with an excellent opportunity to assess if culture in the low-shear environment of the RWV allowed the differentiation of these cells into high-fidelity, 3-D tissue-like masses which more accurately modeled in vivo human intestinal epithelial tissue than did their monolayer counterparts.

In this study, we used the RWV bioreactors to develop novel 3-D cultures of human intestinal epithelial cells which more accurately model the behavior of in vivo tissues than do monolayer cultures of the same cells and thus would be predicted to more closely replicate the complex environment encountered by *Salmonella* during the natural course of human infection. We demonstrate that the 3-D intestinal cells reacted much differently to *Salmonella* infection than did conventional monolayers of the same cell line, including differences in bacterial adherence and invasion, apoptosis, cytokine expression, prostaglandin synthesis, and tissue pathology.

MATERIALS AND METHODS

Bacterial strains and growth conditions. All infectivity studies were performed using wild-type *S. enterica* serovar Typhimurium χ3339, which is an animal-

passaged isolate of the virulent SL1344 wild-type strain (20). Bacterial cells were first grown in Lennox broth (L broth) (30) as static overnight cultures at 37°C. Cultures were then inoculated at a dilution of 1:200 into 50 ml of L broth and subsequently grown with aeration at 37°C until reaching the mid-log phase of growth. Unless otherwise stated, all infectivity studies were performed at a multiplicity of infection (MOI) of between 1 and 10 bacteria per host cell.

Development of a 3-D Int-407 cell culture model. The human embryonic intestinal epithelial cell line Int-407 was obtained from the American Type Culture Collection (CCL-6) (22) and was initially grown in Corning T-75 flasks (2×10^5 cells/ml) at 37°C in a 5% CO_2 environment in preparation for seeding into the RWV. The cells were cultured in a specialized growth medium comprised of a triple-sugar minimal essential medium α–L-15 base supplemented with 6% fetal bovine serum, designated GTSF-2 (18). After 24 h, the spent medium was removed, fresh GTSF-2 was added, and the cells were cultured until reaching approximately 70% confluency. Cells were then washed once with prewarmed calcium- and magnesium-free phosphate-buffered saline, removed from the flask by treatment with 0.25% trypsin, and resuspended in fresh medium at a density of 2×10^5 cells/ml. The cells were assayed for viability by trypan blue dye exclusion. Cells were then introduced into the RWV (Synthecon, Inc.) containing 5 mg of Cytodex-3 microcarrier beads (Pharmacia) per ml, resulting in a final ratio of 10 cells/bead (18). Cytodex-3 microcarriers were type I, collagen-coated dextran beads (average diameter, 175 μm). Cells were cultured in the RWV bioreactors in GTSF-2 at 37°C and 5% CO_2 with initial rotation at 20 rpm. Rotation speed was increased throughout growth to maintain cell aggregates in suspension. Cell growth was monitored daily by measurements of pH and of dissolved CO_2 and O_2 and glucose utilization using a Corning blood gas analyzer (Model 168) and a Beckman Glucose Analyzer-2, respectively. Fresh medium was replenished by 90% of the total vessel volume each 12 to 24 h, depending upon the growth rate of the cultures. As metabolic requirements increased, fresh medium was supplemented with an additional 100 mg of glucose per dl. Immediately prior to use of the 3-D intestinal tissues, fresh medium was added to the cultures. For all studies, 3-D intestinal tissues were cultured in the RWVs for 28 to 32 days prior to their use.

Immunohistochemistry and staining. Int-407 cells cultured as 3-D aggregates or as monolayers were subjected to immunohistochemical characterization. Samples for immunohistochemistry were taken from multiple experiments, fixed, and sectioned as previously described for light microscopy (18) or fixed as previously described for confocal imaging (43). Immunophenotyping was performed on 0.5-μm-thick sections of the 3-D Int-407 tissue aggregates, or monolayer culture controls, after extraction of the epoxy with melting solution (18) for light microscopy studies. Slides of sectioned material were subsequently rehydrated and subjected to immunoperoxidase staining (18) with a panel of antibodies. To evaluate the mucin content, specimens were stained with periodic acid-Schiff stain (PAS) as described previously (7).

Morphological comparisons among normal human small intestine, Int-407 monolayers, and 3-D Int-407 aggregates were determined from paraffin-embedded sections of these samples stained with hematoxylin-eosin and analyzed via light microscopy (3).

Microscopy. For scanning electron microscopy (SEM) analysis, 3-D cell and monolayer samples were fixed in 4% glutaraldehyde. The samples were then immersed in 0.1% osmium tetroxide solution (Electron Microscopy Sciences) and dehydrated in a graded alcohol series to 100% ethanol. The 3-D cell aggregates were placed on a glass coverslip treated with 1% polyethyleneimine. Both 3-D cell cultures and monolayers were chemically treated with hexamethyldisilazane (Electron Microscopy Sciences) and allowed to dry. All cells were then mounted on specimen stubs and sputter coated with gold-palladium for observation in a JEOL 660T or Philips XL-30 series scanning electron microscope.

For confocal imaging, samples were prepared as described previously (43). Confocal imaging was performed using a Zeiss LSM 400 series laser scanning microscope (LSM). Fluorochrome excitation of Alexa 488-labeled secondary antibodies was performed by 488-nm filtered emission from a Kr-Ar laser source. Each image is the compilation of 16 scans of 2 s each, collected at identical exposure levels (the confocal pinhole size, laser output, filter settings, and gain and contrast settings were held constant throughout). Each scan was corrected for background variations and noise by the LSM scanning software during the compilation process. This correction resulted in enhanced resolution but did not affect exposure levels. Postcollection processing of the images was performed using Adobe PhotoShop. As before, no changes in image brightness or contrast were made.

For transmission electron microscopy (TEM) analysis, samples were prepared as described previously (28). TEM imaging was performed using a JEOL 1010 series transmission electron microscope.

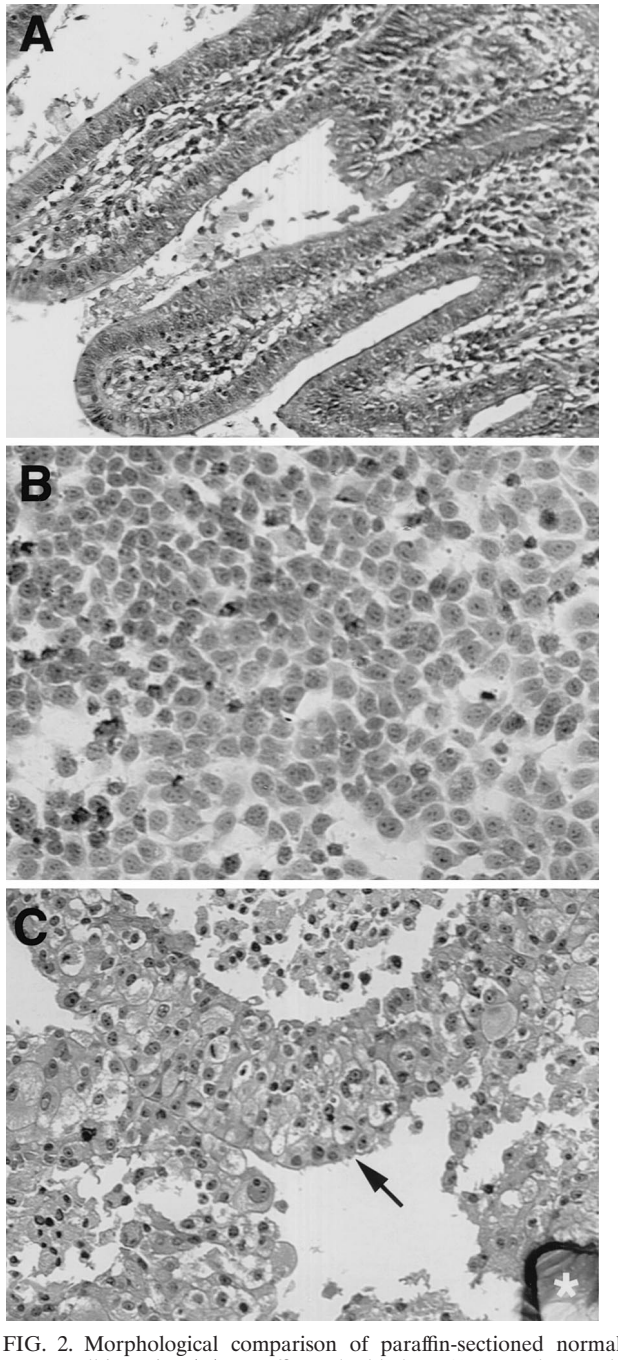

FIG. 2. Morphological comparison of paraffin-sectioned normal human small intestine (A), paraffin-embedded Int-407 monolayer cultures (B), and paraffin-sectioned Int-407 3-D aggregates (C) stained with hematoxylin-eosin. Note the clear, 3-D organization observed in a cross section of an Int-407 3-D-construct (C, arrow), morphologically reminiscent of the intestinal villi seen in normal small intestine (A). In contrast, note the complete lack of organization observed when Int-407 cells are cultured as standard monolayers (B). A sectioned microcarrier bead can be seen in panel C (asterisk). All micrographs were obtained at an 200 ×magnification.

Adherence and invasion assays. Adherence and invasion assays were conducted as described previously (37), with the modification that 3-D Int-407 cells were seeded into 24-well tissue culture plates for infectivity assays. The number of cells associated with 3-D aggregates was initially determined by counting released nuclei as described previously (18). As a confirmation of the number of cells counted by released nuclei, cells in the 3-D aggregates were also counted by

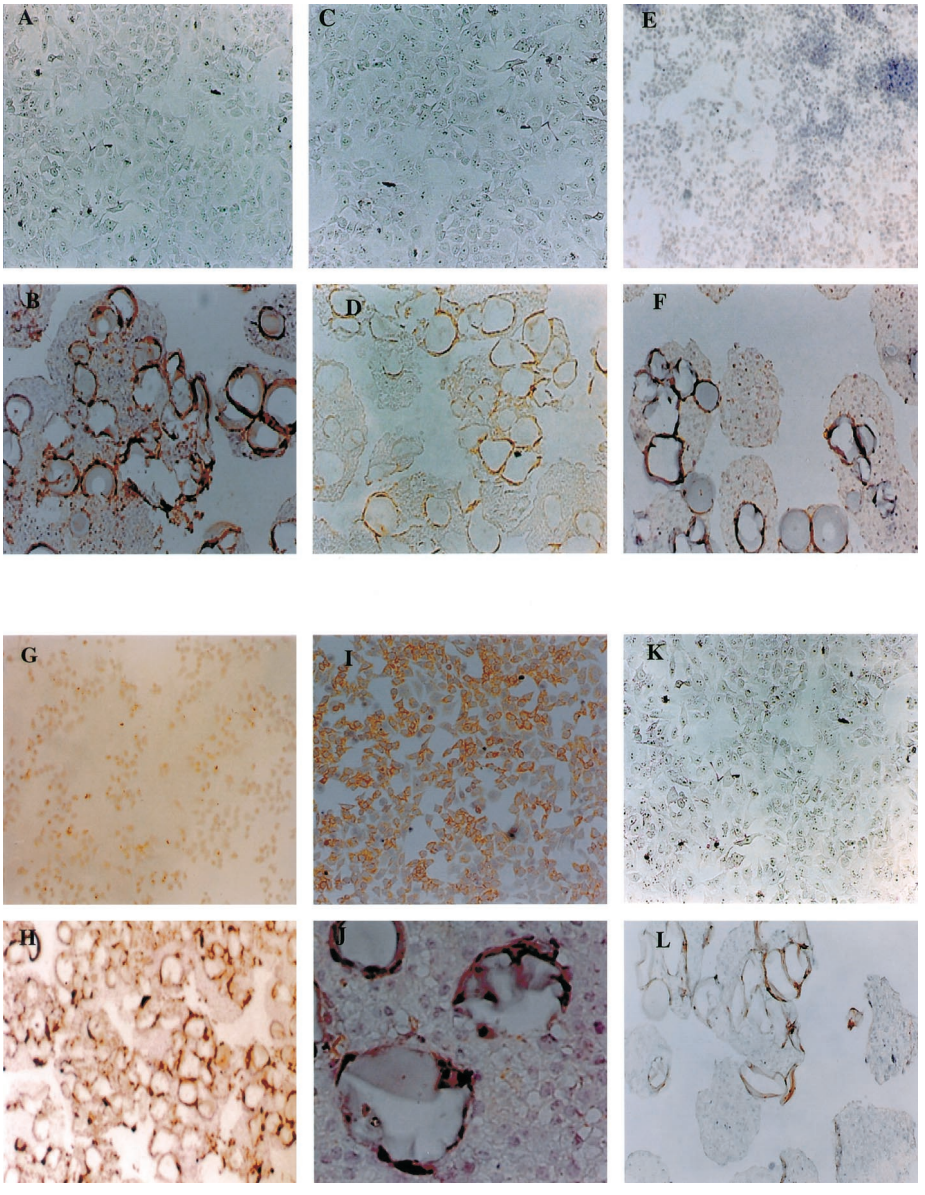

FIG. 3. Immunohistochemical analysis of 3-D Int-407 aggregates compared to Int-407 monolayers. This figure demonstrates positive staining in 3-D Int-407 tissue aggregates for collagen type II, fibronectin, sialyl Lewis A, and villin (B, D, F, and H, respectively) (×100) and the absence of staining for cytokeratin 18 (J) compared to Int-407 monolayers stained for the same markers (A, C, E, G, and I, respectively) (×100). Antibody-negative controls for 3-D tissue aggregates and monolayers (K and L, respectively) (×100) demonstrate a total lack of staining. For reference, circular and oval lumenal areas seen in the photos are cross sections of microcarrier spheres around which cellular material is growing.

dissociation into individual cells by treatment with 0.1% EDTA. The cell number and viability were determined by trypan blue dye exclusion.

Analysis of cytokine expression of Int-407 cells following *Salmonella* infection. The cytokine mRNA profiles expressed following *Salmonella* infection of 3-D Int-407 tissue aggregates and Int-407 monolayers were analyzed and quantified using a commercially available multiprobe RNase protection assay (RiboQuant; PharMingen, San Diego, Calif.). Total RNA isolated from uninfected and infected 3-D intestinal aggregates and Int-407 monolayers was extracted using TriReagent in an acid guanidinium thiocyanate-phenol-chloroform method according to the manufacturer's instructions (Molecular Research Center, Inc., Cincinnati, Ohio). Total RNA was then used in RNase protection assays with a mixture of [^{32}P]UTP-labeled antisense riboprobes generated from a panel of different human cytokine templates, specifically in this case tumor necrosis factor alpha (TNF α), interleukin 1α (IL-1α), IL-1β, TNF-β, lymphotoxin β, gamma interferon, alpha interferon, IL-6, IL-10, IL-12, IL-18, and transforming growth factor β (TGF-β1). The template mixtures containing these cytokine templates also included templates for the housekeeping genes encoding glyceraldehyde-3-phosphate dehydrogenase (GAPDH) and L32 (a ribosomal protein) to ensure equal loading of total RNA onto 6% polyacrylamide–7 M urea gels.

Quantification of each mRNA was accomplished with a Fuji FLA-3000 PhosphorImager and ImageGauge software. Each mRNA band was normalized to L32 or GAPDH from the same RNA sample, and the data are presented as arbitrary units of each given cytokine.

Prostaglandin immunoassays. Levels of prostaglandin E_2 (PGE_2) were determined in culture supernatants of infected and uninfected 3-D Int-407 cells seeded into 24-well tissue culture plates and of Int-407 monolayers by enzyme immunoassay according to the manufacturer's instructions (R&D Systems). Bacteria were prepared for infections as described above with an MOI of 50:1 to 100:1. All Int-407 cells were infected for 1 h with χ3339 and cultured for an additional 7 h in the presence of gentamicin (10 μg/ml) to kill any remaining extracellular bacteria. Culture supernatants were sampled for PGE_2 expression prior to addition of *Salmonella* and at 1, 2, and 8 h following infection.

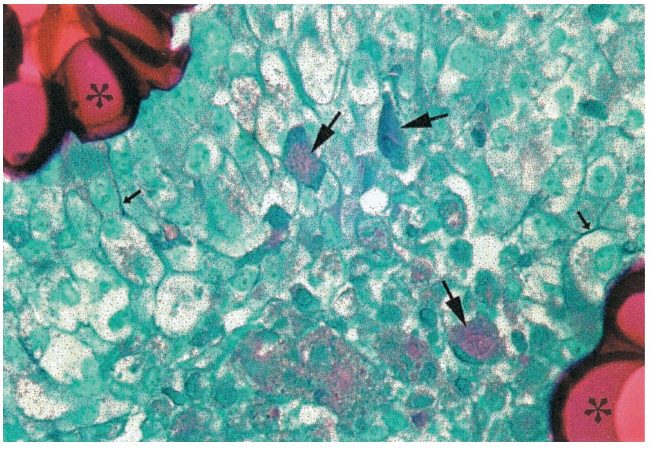

FIG. 4. PAS of paraffin sections of Int-407 3-D constructs. Note the presence of isolated PAS-positive cells (large arrows) surrounded by PAS-negative cells. Cytodex beads (asterisks) and some discrete areas of extracellular matrix (small arrows) also exhibit a positive reaction with the PAS. The presence of a differential PAS pattern in paraffin sections of 3-D constructs suggests the presence of a mucus-producing subpopulation of cells within the construct.

Apoptosis analysis. Following incubation for 1.5 h with or without *Salmonella*, Int-407 monolayers and 3-D aggregates were dissociated into individual cells by treatment with 0.1% EDTA. The cell number and viability were determined by trypan blue dye exclusion. The resulting single cell suspensions were washed with calcium-containing phosphate-buffered saline and incubated for 15 min with fluorescein isothiocyanate-conjugated annexin V (R&D Systems) and/or propidium iodide to quantitate apoptosis and necrosis, respectively. Positive controls for apoptosis and necrosis were cultures of 3-D Int-407 tissue aggregates or monolayers cultured with actinomycin D (1 μg/ml) and sodium azide (1.0%), respectively. These control cells were incubated with actinomycin D or sodium azide for 2 to 3 h prior to washing and staining with fluorescein isothiocyanate-annexin V and propidium iodide and analysis on a FACSVantage flow cytometer.

RESULTS

Immunohistochemical characterization of cultured cells. Characterization of the in vivo epithelial cell expression characteristics of the RWV-grown intestinal 3-D aggregates relative to monolayer cultures was performed by examining immunohistochemical and proto-oncogene expression patterns of histological sections of these cultured cells. Immunohistochemical analysis was performed on histological sections of tissue obtained from the RWV and monolayer controls with antibodies against collagens II and III, fibronectin, vimentin, pancytokeratin, sialyl Lewis A (M-cell marker), villin, and cytokeratin 18. Immunohistochemical analysis of 3-D Int-407 tissue aggregates and Int-407 monolayers revealed striking differences between the two cultures. In general, the 3-D intestinal aggregates demonstrated tissue organization similar to that found in vivo (Fig. 2C and A, respectively), while monolayer material showed poor organization (Fig. 2B), reduced expression of specific markers normally present in differentiated human intestinal epithelium, and reduced expression of the differentiated phenotype. Specifically, 3-D aggregates of Int-407 cells exhibited very strong staining for the extracellular matrix proteins collagen type II (Fig. 3B) and fibronectin (Fig. 3D), compared to weakly to moderately positive staining for these same epitopes in Int-407 monolayers (Fig. 3A and C, respectively). In addition, expression of the M-cell glycoconjugate sialyl Lewis A antigen was also enhanced in the 3-D aggregates (Fig. 3F) relative to the monolayers (Fig. 3E). 3-D aggregates also exhibited increased staining for the cytoskeletal marker villin (an abundant protein in the brush border epithelial cells of the small intestine) (Fig. 3H), compared to the weaker staining for this epitope observed in Int-407 monolayers (Fig. 3G). Interestingly, expression of cytokeratin 18, a marker associated with tumor, abnormal, and undifferentiated cells, was significantly down-regulated in the 3-D aggregates (Fig. 3J) compared to monolayers (Fig. 3I). Moreover, the 3-D aggregates also exhibited enhanced staining for collagen III, vimentin, and pancytokeratin compared to monolayers (data not shown). Negative controls for all immunohistochemical analyses are shown in Fig. 3K (monolayers) and 3L (3-D aggregates). In addition, histochemical staining with PAS showed mucins to be produced by the 3-D Int-407 aggregates (Fig. 4) but not by monolayers (data not shown).

Characterization of the in vivo epithelial cell expression characteristics of the intestinal 3-D aggregates relative to monolayer cultures was further studied via immunohistochemical analysis by whole-mount confocal microscopy of tissue obtained from the bioreactor and monolayer controls with antibodies against type IV collagen, laminin, cadherin, epithelium-specific antigen (ESA), and cytokeratin 7, all of which are proteins that serve as widely accepted markers of epithelial differentiation. Immunostaining for ESA, an antigen expressed only in epithelia, indicated that the Int-407 cells were indeed epithelial in nature. All cells in both the monolayer cultures and the 3-D epithelial constructs expressed this antigen (Fig. 5B and A, respectively). Confocal microscopy of the cell surface ESA showed how densely populated the interstices of the stratified epithelioid 3-D constructs were with closely adherent layers of cells—a finding quite divergent from that seen in monolayer culture (Fig. 5A and B, respectively).

As epithelia form, the cells adhere to each other via lateral cell-cell interactions mediated by a class of plasmalemmal binding proteins known as the cadherins. Developmentally mature epithelia display a very tight association of cadherins to their lateral surfaces in the areas where they adhere to other cells. Ultrastructurally, this zonula adherens is easily identified as a band of actin filaments decorated with dense accumulations of cadherin protein. The 3-D Int-407 cultures showed just such a dense, regular appearance of the cadherin assemblies along their lateral cell-cell boundaries (Fig. 5C). By comparison, the monolayer cultures displayed copious cadherin accumulations only in areas containing closely proximated cells, areas that occur with much less frequency (Fig. 5D). This indicated that the 3-D culture constructs have very well defined lateral cell-cell borders and junctional complexes throughout, while the monolayer cultures appear to still be in the process of initiating lateral polarity in a large proportion of the cell population.

In comparison to Int-407 cells grown as monolayers in culture, the expression of laminin (Fig. 5I and J) and type IV collagen (Fig. 5K and L) was noticeably up-regulated. Both of these proteins are known to contribute to formation of the basal lamina, a structural component of all developmentally mature and fully functional epithelia. Developmentally, the basal lamina is deposited at the cell-substrate interface of a nascent epithelium defined only by lateral cell-cell adhesions,

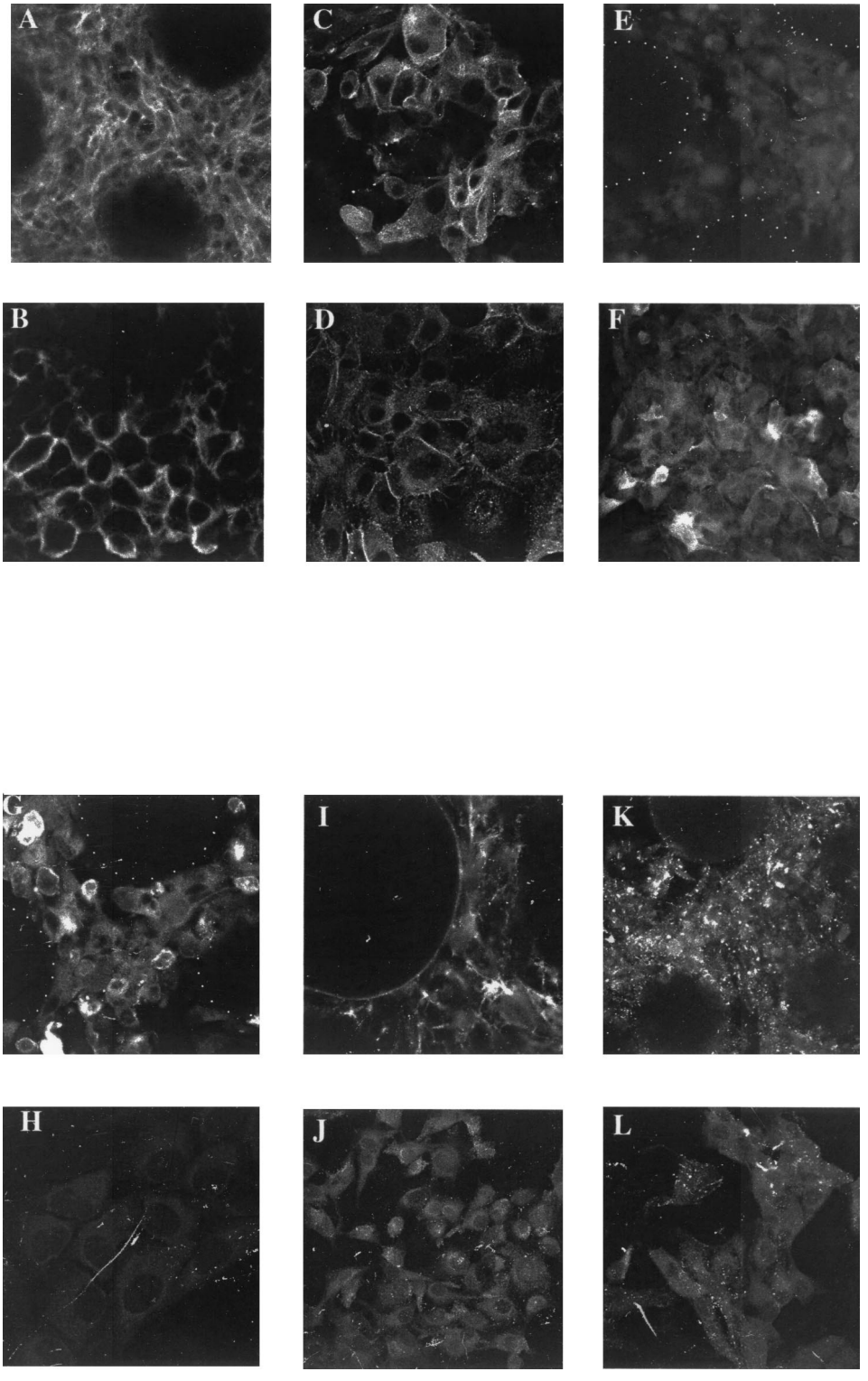

FIG. 5. Confocal images of antibody-stained Int-407 monolayers and 3-D constructs. Confocal images of Int-407 cells grown as monolayers (B, D, F, H, J, and L) and 3-D aggregates (A, C, E, G, I, and K) stained with monoclonal antibodies against ESA (A and B), cadherin (C and D), cytokeratin 19 (E and F) (note that the 150-μm beads are delineated by a dotted outline in panel E), cytokeratin 7 (G and H) (note that the 150-μm beads are delineated by a dotted outline in panel G), laminin (I and J), and collagen type IV (K and L).

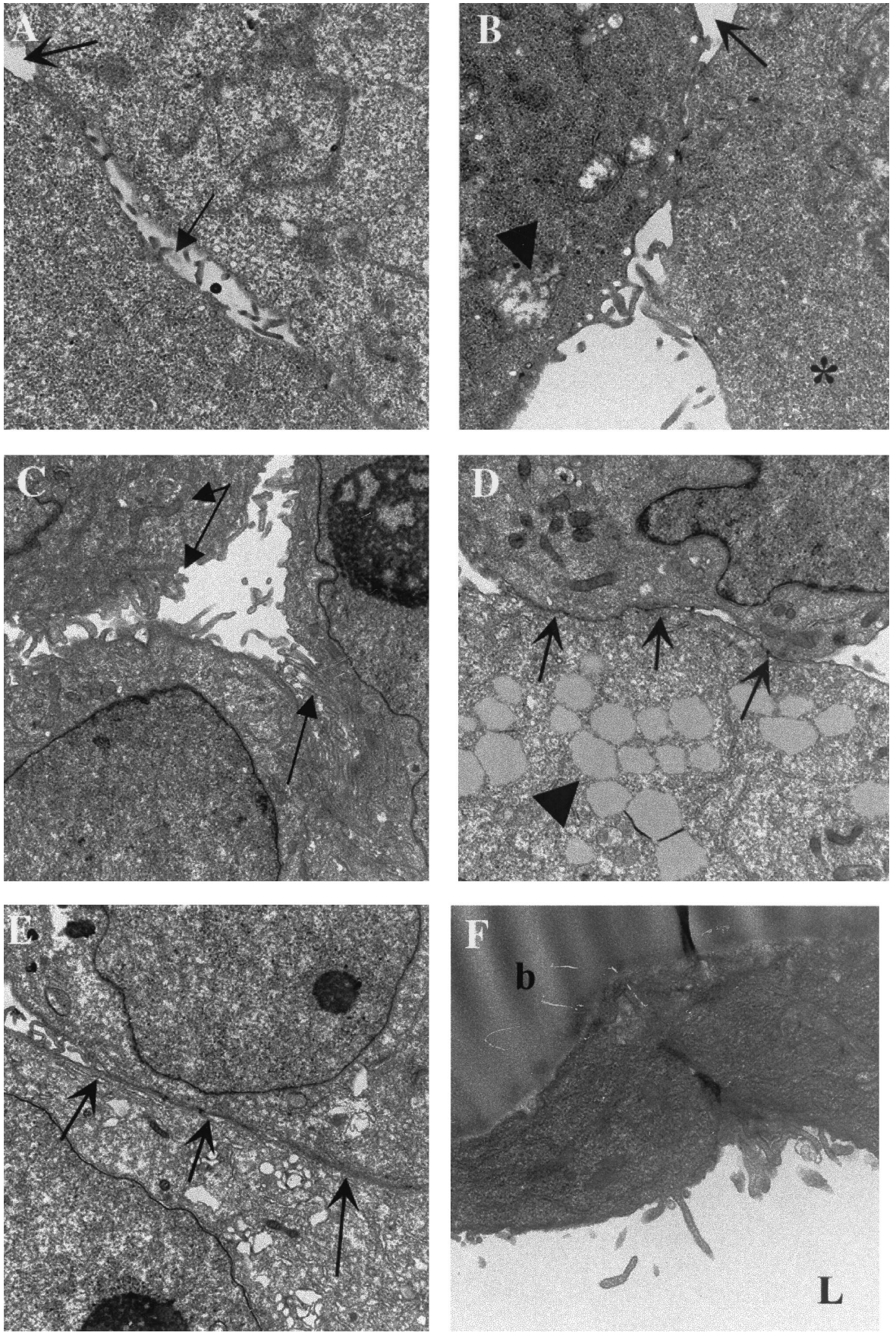
A
B
C
D
E
F
b
L

thus imparting an apical-basal polarity to the entire structure. In 3-D Int-407 cultures, the presence of these basal laminal proteins, and their deposition at the cell-substratum interface, is highly indicative of the first stages in the formation of apical-basal polarity (Fig. 5I and K, respectively).

Finally, we studied the expression and histological pattern of a group of cytoskeletal proteins, the cytokeratins. Cytokeratin 19, a marker associated with tumor and abnormal cells, was dramatically down-regulated in the 3-D aggregates (Fig. 5E) (note that 150-μm beads are delineated by a dotted outline in the figure) compared to monolayers (Fig. 5F). Conversely, cytokeratin 7, absent in the monolayer cultures (Fig. 5H) was up-regulated by 3-D culture conditions (Fig. 5G). While we are not yet sure what this cytokeratin modulation means with respect to the functional specificity of the 3-D constructs, we can consider this finding indicative of large-scale phenotypical alterations associated with 3-D culture.

TEM analysis. Characterization of the in vivo epithelial cell expression characteristics of the 3-D intestinal aggregates relative to monolayer cultures was further examined using TEM analysis. Overall, monolayer cultures demonstrated poor structural and functional fidelity compared to their 3-D counterparts. Specifically, monolayer cultures exhibited irregular microvillus development (Fig. 6A), significant cellular granularity (Fig. 6B) accompanied by minimal tight junction formation (Fig. 6A and B), poorly formed glandular and/or vacuole-like formation (Fig. 6B), lack of apical polarity, and poorly formed desmosomes (Fig. 7). In contrast, 3-D cultures demonstrated well-developed and abundant microvilli (Fig. 6C) which were apically oriented (Fig. 6F); well-formed tight junctions (Fig. 6D and E); numerous, well-formed vacuole-like structures (Fig. 6D); and well-formed desmosomes (Fig. 7).

Adherence and invasion assays. An initial step in the pathogenesis of *Salmonella* infection is the adherence and entry of these organisms into the intestinal epithelium. Accordingly, we examined the ability of serovar Typhimurium χ3339 to adhere to and invade 3-D tissue aggregates of Int-407 cells compared to Int-407 monolayers. Representative data from three trials showed that, with respect to the percentage of initial inoculum (MOI of 10:1), the adherence and invasion of *Salmonella* into 3-D Int-407 cells (2.6 ± 1.3 and 1.3 ± 0.8, respectively) was significantly lower than that observed for Int-407 monolayers (48.0 ± 19.0 and 51.0 ± 18.0, respectively). The adherence and invasion numbers observed in this study for χ3339 for the Int-407 monolayers are consistent with those published previously (37).

Pathology of 3-D tissue aggregates relative to monolayers before and after infection with *Salmonella*. SEM was used to examine surface interactions and membrane structural alterations which occurred over time following *Salmonella* infection of 3-D Int-407 aggregates compared to monolayers. Observations of numerous samples revealed major changes in the integrity of the monolayers compared to 3-D intestinal tissues following time course infections with *Salmonella* at the same MOI. At time zero, SEM revealed typical, young confluent monolayers (Fig. 8A). As early as 10 min postinfection, observable differences in structural integrity were observed in the Int-407 monolayers compared to uninfected controls, the former showing extensive formation of membrane blebs and several areas of protruding cytoplasm resembling membrane ruffles (Fig. 8B), as observed previously for serovar Typhimurium (reviewed in reference 17). One hour postinfection, the Int-407 monolayers appeared swollen with membrane blebs and the formation of pathological lesions (Fig. 8C). There was a dramatic loss of structural integrity of the monolayers at 2 h postinfection, including the presence of extensive lesions, as well as large swollen areas of denuded surface membrane (Fig. 8D).

Three-dimensional Int-407 tissue aggregates infected with *Salmonella* did not display as extensive a loss of structural integrity as that observed for infected Int-407 monolayers following the same time course of infection. At time zero (i.e., uninfected control), SEM revealed dense masses of cells associated with the microcarrier beads with apparent mucus-like extracellular secretions covering the cells. Note the fuzzy appearance of what appears to be mucus present on the epithelial cell aggregates (Fig. 9A). Ten minutes postinfection, the surface of the 3-D Int-407 cells appears slightly irritated; however, unlike the infected monolayers, few bacteria are observed in association with the surface of the 3-D aggregates (Fig. 9B). One hour postinfection, numerous depressed and/or pitted areas are evident, which are devoid of mucus-like extracellular secretions (Fig. 9C). By 2 h postinfection, numerous lesions are apparent on the surface of the 3-D Int-407 cells. In addition, regions of membrane blebbing are also abundant (Fig. 9D).

Analysis of cytokine expression of human intestinal epithelial cells following *Salmonella* infection. To characterize the cytokine expression of 3-D Int-407 aggregates compared to monolayer cultures following infection with serovar Typhimurium, we used a commercially available multiprobe RNase protection assay to quantify and compare the cytokine mRNA profiles. Infection of both Int-407 monolayers and 3-D aggregates with serovar Typhimurium resulted in significantly increased expression of TNF-α, IL-6, IL-1α, IL-1β, and IL-1Ra at 1 and 2 h after infection compared to uninfected monolayers and 3-D aggregates, respectively. Representative data are shown for TNF-α (Fig. 10A) and IL-6 (Fig. 10B). Infection of Int-407 monolayers with *Salmonella* induced significantly increased expression of TNF-α at 1 h after infection ($P < 0.0005$) and at 2 h after infection ($P < 0.0001$) compared to uninfected

FIG. 6. Transmission electron micrographs of 3-D Int-407 aggregates compared to Int-407 monolayers. This figure demonstrates TEM images of Int-407 monolayers (A and B) and 3-D Int-407 cells (C to F). Note the poorly developed and sparse microvilli observed in the monolayers (A) compared to the well-developed and abundant microvilli in the 3-D aggregates (L) (solid arrows). In addition, the monolayers showed high levels of cellular granularity (B, asterisk) indicative of poorly differentiated cells. Moreover, the monolayers (A and B) demonstrated inferior tight junction formation compared to the 3-D aggregates (D and E) (concave arrows). Panel E shows the formation of tight junctions which run nearly the length of the margin between two 3-D cells (concave arrows). Note the presence of numerous, well-formed vacuole-like structures in the 3-D aggregates (D) compared to their poorly developed counterparts in the monolayers (B) (arrowheads). In panel F, two Cytodex microcarrier beads (b) can be seen which are partially covered with 3-D cells. Note the apical orientation of the microvilli toward the luminal (L) side.

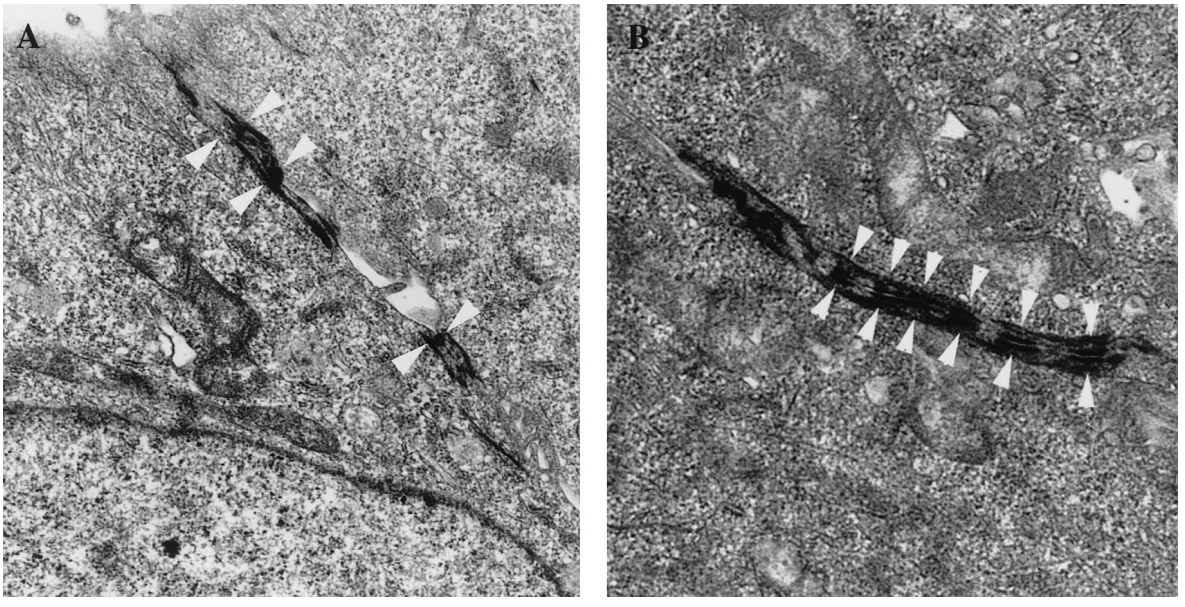

FIG. 7. Transmission electron micrographs of desmosome formation in the 3-D Int-407 aggregates compared to monolayers. This figure demonstrates TEM images of Int-407 monolayers (A) and 3-D Int-407 cells (B), showing well-formed and extensive desmosome formation in the latter. The desmosomes consist of two opposing dense plaques on the cytoplasmic membranes (shown by arrowheads). Note the poorly formed and incomplete nature of the desmosomes in the monolayers.

monolayers (Fig. 10A). TNF-α mRNA levels were significantly elevated at 1 h ($P < 0.0005$) and 2 h ($P < 0.0001$) after infection of 3-D aggregates compared to uninfected 3-D aggregates; however, TNF-α expression did not increase from 1 h after infection to 2 h after infection (Fig. 10A). Although infection of both Int-407 monolayers and 3-D aggregates resulted in increased TNF-α mRNA levels, TNF-α expression was more than fivefold higher in the monolayers at 2 h after infection than in the 3-D aggregates. Similarly, infection with serovar Typhimurium induced expression of IL-6 in both Int 407 monolayers and 3-D aggregates (Fig. 10B). Significantly higher levels of IL-6 mRNA were detected at 1 h ($P < 0.002$) and 2 h ($P < 0.0001$) after infection of Int-407 monolayers compared to uninfected monolayers. Infection of Int-407 monolayers resulted in greater than a 50-fold increase in IL-6 transcription at 2 h after infection compared to uninfected monolayers (Fig. 10B). Although IL-6 transcription in Int-407 3-D aggregates was significantly higher at 2 h after infection ($P < 0.005$) compared to uninfected 3-D aggregates, the overall increase was just over threefold in magnitude.

Transcription of IL-1α, IL-1β, and IL-1Ra was also elevated following infection of Int-407 monolayers and 3-D aggregates (data not shown). In each case, constitutive expression was higher in uninfected 3-D aggregates than in monolayers. By 2 h after infection of monolayers, IL-1α expression increased by 17-fold compared to uninfected monolayers and IL-1β expression increased by 13-fold, whereas expression of the IL-1 inhibitor, IL-1Ra, increased by just over 3-fold. In contrast, 2 h after infection of 3-D aggregates, IL-1α expression increased fourfold and IL-1β expression increased approximately threefold while expression of IL-1Ra was increased twofold compared to uninfected 3-D aggregates. Taken together, it appears that IL-1α and IL-1β expression is up-regulated more in Int-407 monolayers than in 3-D aggregates, whereas expression of the IL-1 inhibitor, IL-1Ra, is increased about the same in monolayers as in 3-D aggregates following infection with serovar Typhimurium. Thus, proinflammatory effects of IL-1α and IL-1β may be more prominent in the Int-407 monolayers following infection with serovar Typhimurium than in the 3-D aggregates.

TGF-β1 frequently serves in an immunosuppressive role (27); thus, we examined expression of this cytokine following infection of Int-407 monolayers and 3-D aggregates. Although infection with serovar Typhimurium did not significantly affect expression of TGF-β1 at 1 or 2 h after infection of either monolayers or 3-D aggregates, TGF-β1 mRNA levels were always twofold higher in the 3-D aggregates than in the monolayers (data not shown).

Assay for apoptosis of human intestinal epithelial cells after *Salmonella* infection. When grown as monolayers, several cell lines have been shown to undergo apoptosis following *Salmonella* infection (4, 25). To assess the relationship between bacterial infectivity and death of human intestinal Int-407 cells cultured in the RWV or as monolayers, we used flow cytofluorometry to characterize apoptotic cell death of these cells before and after *Salmonella* infection. Following 1.5 h of infection with *Salmonella*, Int-407 monolayers contained approximately eightfold more apoptotic cells (68.3%) than did control uninfected monolayers (8.8%). In contrast, there was no increase in apoptosis following the same time course of *Salmonella* infection of 3-D Int-407 aggregates, with a 5.2 and 7.3% apoptotic index of aggregates pre- and postinfection, respectively.

Prostaglandin production by *Salmonella*-infected and uninfected human intestinal epithelial cells. Increased prostaglandin synthesis from epithelial cells following *Salmonella* infection in vitro has previously been demonstrated (9). To determine whether there was a differential induction of pros-

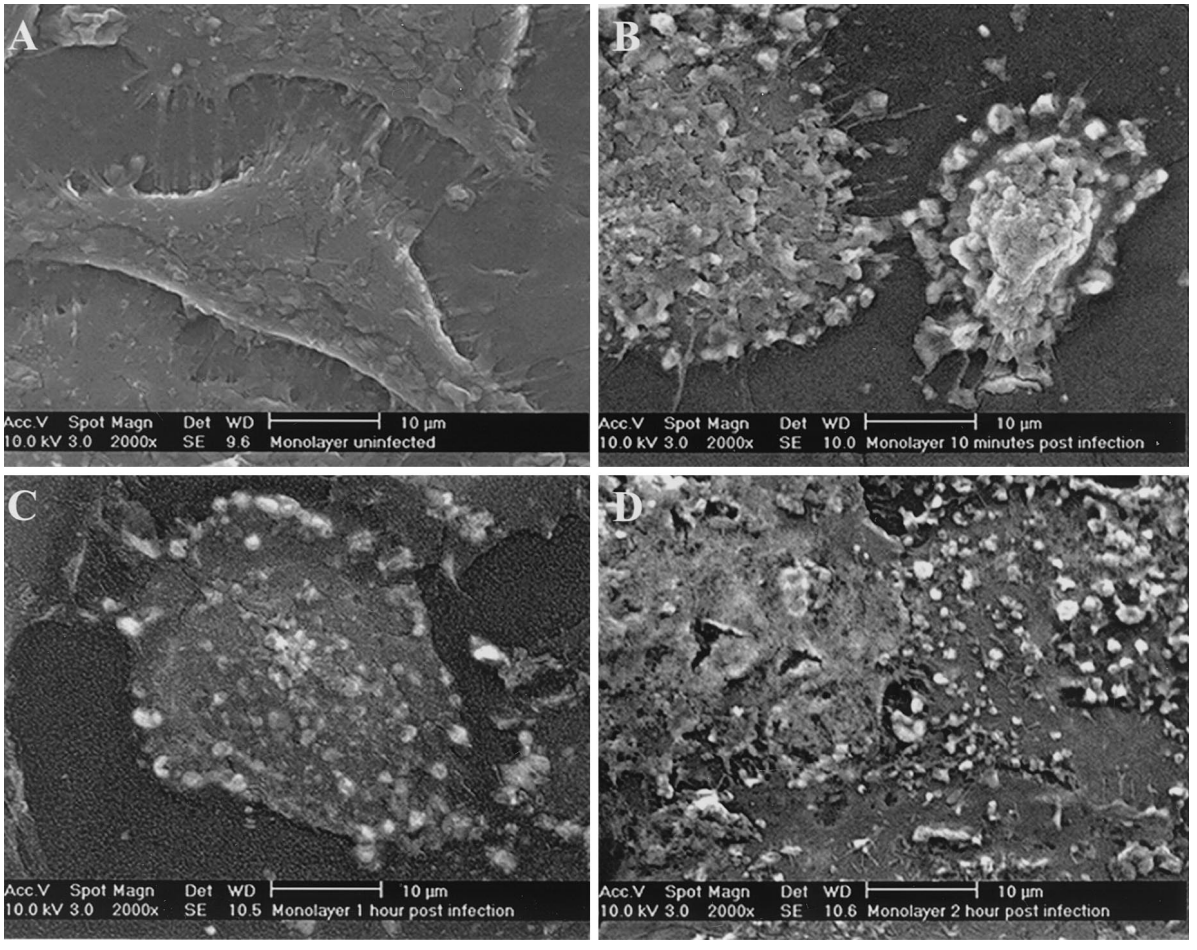

FIG. 8. Scanning electron micrographs of *Salmonella* interaction with Int-407 monolayers. Shown are electron micrographs of uninfected and infected Int-407 monolayers (×2,000). (A) Uninfected monolayer control. (B) Monolayer at 10 min postinfection (at an MOI of 10:1), showing major surface alterations, including extensive formation of membrane blebs and several surface structures resembling membrane ruffles. (C) By 1 h postinfection, the Int-407 cell surface appears swollen and denuded with membrane blebs. (D) At 2 h postinfection, Int-407 cells exhibit a loss of structural integrity with numerous membrane alterations including blebs and the formation of pathological lesions, as well as some surface-bound bacteria.

taglandin synthesis in response to *Salmonella* infection between the Int-407 cells cultured as 3-D aggregates and those cultured as monolayers, we measured PGE_2 levels in these cells by immunoassay before and after infection with χ3339. Levels of PGE_2 were not increased in 3-D Int-407 cells or in monolayers following *Salmonella* infection at 1, 2, or 8 h (Table 1). In contrast, there was a significant increase in the level of constitutive PGE_2 synthesis (approximately 79-fold) in the uninfected 3-D Int-407 cells compared to monolayer cultures (Table 1).

DISCUSSION

In this study, we used a novel class of rotating bioreactors, which are optimized to minimize shear and turbulence, to culture 3-D human intestinal epithelial tissue retaining many differentiated features as a model to study the infectivity of the enteroinvasive pathogen *Salmonella*. Our results indicate that the 3-D cultured human intestinal cells more accurately model in vivo tissues than do monolayer cultures of the same cells and thus more closely replicate the complex environment encountered by *Salmonella* during the natural course of human infection. These observations are characterized by important differences between the 3-D Int-407 cells and Int-407 monolayers in response to infection with *Salmonella*, including differences in adherence, invasion, apoptosis, prostaglandin synthesis, and tissue pathology.

Studies of the intestinal 3-D aggregates and monolayer cultures via fluorescent and whole-mount confocal microscopy using proteins that serve as widely accepted markers of epithelial differentiation revealed a number of important distinctions between the two culture conditions. In general, histological sections of the 3-D intestinal aggregates revealed tissue organization and differentiation similar to that found in vivo, while monolayer material showed poor organization, reduced expression of specific markers normally present in differentiated human intestinal epithelium, and reduced expression of the differentiated phenotype. The increased expression by 3-D aggregates of extracellular and basement membrane proteins, specific epithelial and endothelial cell markers, and mucin indicates important aspects of differentiated tissues and sug-

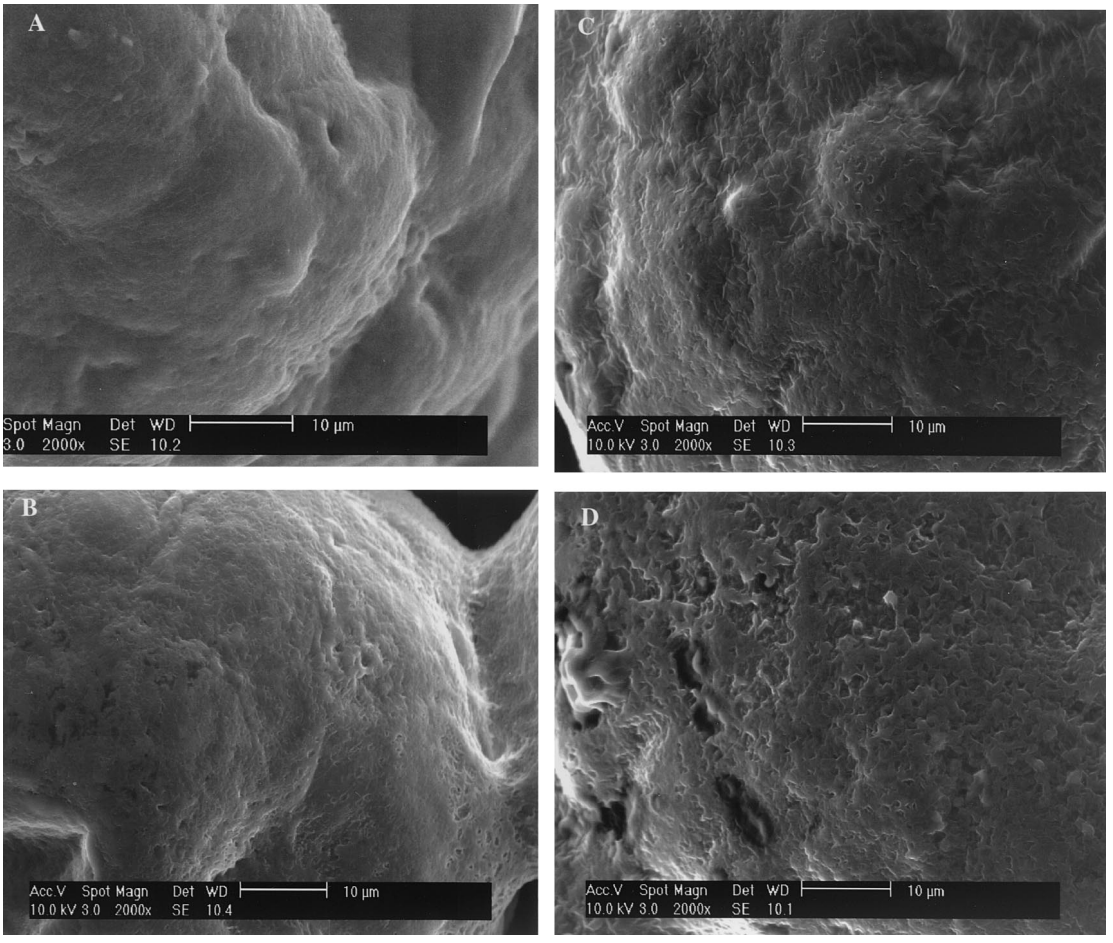

FIG. 9. Scanning electron micrographs of uninfected and infected 3-D Int-407 aggregates. Shown are electron micrographs of uninfected and infected 3-D Int-407 aggregates in the RWV (×2,000). (A) Uninfected 3-D Int-407 control showing dense masses of cells with extracellular secretions. (B) 3-D Int-407 aggregates at 10 min postinfection (at an MOI of 10:1), showing minor irritation on the Int-407 apical cell membrane. (C) By 1 h postinfection, numerous surface depressions and/or membrane blebs are apparent on the 3-D Int-407 cells, with depressed regions devoid of mucus-like secretions. (D) At 2 h postinfection, the surface of the 3-D Int-407 cells is quite irregular and associated with what appear to be numerous surface lesions. Note that few surface-bound bacteria were observed at any of the above postinfection times.

gests that the 3-D cell aggregates have the ability to organize and develop into complex tissue assemblies capable of expressing in vivo-like functional characteristics. The enhanced expression by 3-D aggregates of sialyl Lewis A suggests that the M-cell glycosylation pattern expressed on the surface of the 3-D Int-407 aggregates grown in the RWV may present an epithelial surface to the infecting microbe which more closely resembles that encountered within the host during infection, relative to the Int-407 monolayers. This finding is of particular relevance, since numerous pathogens in addition to *Salmonella* demonstrate a tropism for M cells. However, no continuous M-cell line is currently available. The expression of distinct glycoconjugates by normal human Peyer's patch M cells suggests an important role for carbohydrate epitopes in the function of this unique epithelial cell type. The structural modifications of the M-cell apical surface and the display of particular oligosaccharides together would allow M cells to present a conspicuously unique biochemical face to the lumen which might facilitate adherence, uptake, and immunological sampling of microorganisms (13). Interestingly, expression of cytokeratins 18 and 19, markers associated with tumor, abnormal, and undifferentiated cells, was significantly down-regulated in the 3-D aggregates compared to monolayers. The decreased expression of cytokeratin 18 is suggestive of a shift from a relatively undifferentiated state (as in the monolayers) to the differentiated phenotype observed for the 3-D tissue aggregates. In addition, the 3-D constructs contained a mucus-producing subpopulation of cells that expressed a differential phenotype compared to the surrounding cells. This differential staining pattern is very similar to that observed for mucus-secreting goblet cells within paraffin-fixed sections of intestinal tissue. The presence of a subpopulation of PAS-positive cells in the 3-D Int-407 cell constructs, and not in the monolayers, suggests strongly that culture of these cells in the bioreactor as 3-D, multicellular constructs results in the expression of differential cellular phenotypes, one of which apparently is a mucus-producing cell type, and represents another important similarity to the intestinal mucosa.

Both culture types expressed ESA and cadherin on the cell surfaces; the stratified epithelioid 3-D constructs express a

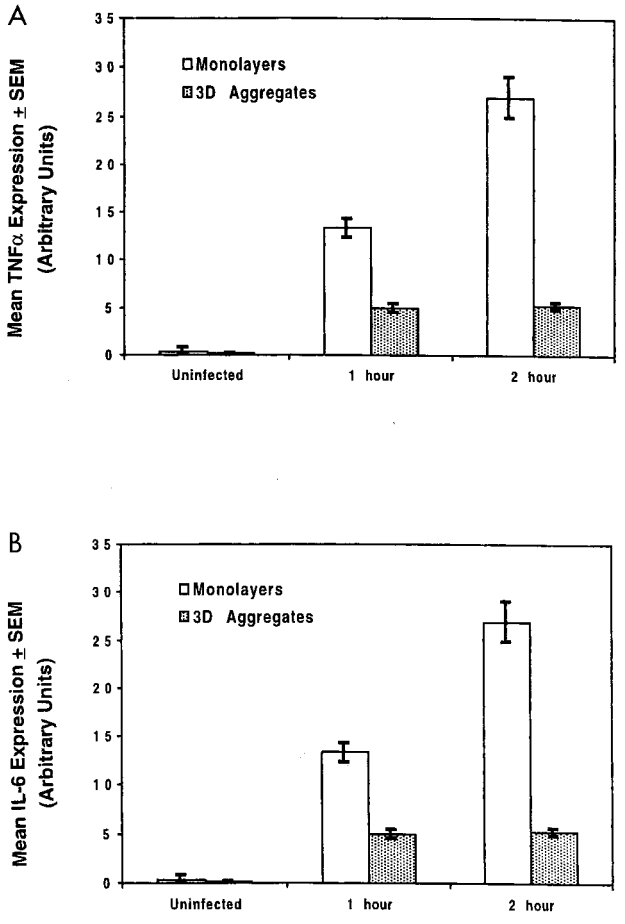

FIG. 10. Cytokine expression of Int-407 monolayers and 3-D tissue aggregates following *Salmonella* infection. Total RNA was isolated from Int-407 monolayers and 3-D tissue aggregates prior to infection with *Salmonella* and at 1 and 2 h after infection. Five micrograms of total RNA from each sample was hybridized individually with radiolabeled riboprobes specific for TNF-α (A) or IL-6 (B) and subjected to RNase protection assay. PhosphorImager technology was used to quantify the levels of transcription of each cytokine and the housekeeping gene GAPDH. Levels of TNF-α and IL-6 transcripts were normalized using GAPDH transcription levels of the same RNA sample, and the levels are displayed as arbitrary units. Four to five replicates of each condition were used to generate means and standard errors of the means (SEM).

much greater amount of these proteins. Furthermore, the proteins are localized specifically to cell-cell interfaces within the closely adherent cell layers of 3-D cultures. This finding indicates that the 3-D culture constructs have well-defined lateral cell-cell borders and junctional complexes throughout, while the monolayer cultures appear to possess nascent lateral polarity in a large proportion of the cell population. The expression of the basal lamina proteins type IV collagen and laminin was up-regulated in the 3-D cultures compared to monolayers. During the development of polarity in the epithelial phenotype, the basal lamina is deposited at the cell-substrate interface of a nascent epithelium following the establishment of strong lateral polarity within that epithelium. In 3-D Int-407 cultures, which already possess well-established lateral polarity, the up-regulated synthesis of basal laminal proteins is highly indicative of the first stages in the formation of apical-basal polarity. Furthermore, the deposition of these proteins at the cell-substrate interface, in this case the surface of the Cytodex microcarrier beads, indicates that the 3-D cultured cells are setting up apical-basal polarity by constructing a nascent basal lamina on their substrate.

Moreover, the 3-D intestinal aggregates exhibited well-formed and numerous microvilli at their apical cell surfaces, abundant and well-developed vacuole-like formation, extensive and well-formed tight junctions, and desmosomes. In summary, the 3-D Int-407 aggregates more closely resemble human differentiated intestinal epithelium than do conventional monolayer cultures of the same cells. As such, 3-D Int-407 cultures would be predicted to more closely replicate the complex environment encountered by *Salmonella* during the natural course of human infection.

Results from infectivity studies demonstrated that *Salmonella* established infection of the 3-D human intestinal cells in a different manner from that of monolayer cultures. *Salmonella* exhibited significantly reduced abilities to adhere to and invade the 3-D human intestinal aggregates compared to monolayer cultures. In agreement with this finding, SEM analysis revealed fewer *Salmonella* bacteria associated with the surface of the 3-D aggregates compared to monolayers. This may be a reflection of the differential expression of host cell surface adhesins by the 3 D Int-407 cells, which are more relevant to the in vivo setting than is growth as monolayers. It is important to note that, in the infected 3-D cells, *Salmonella* invasion can proceed through the external epithelial cells of the aggregates and into the underlying cells. Our invasion studies were conducted for a 2-h period, and thus the bacteria would have had ample time to invade the deeper tissues of the aggregate. However, *Salmonella* exhibited significantly reduced abilities to invade the 3-D human intestinal aggregates compared to monolayers. There is compelling evidence in the literature to suggest that the lower levels of *Salmonella* invasion observed for the 3-D aggregates compared to the monolayers may be physiologically relevant to

TABLE 1. PGE_2 production by Int-407 cells before and after infection with *Salmonella*[a]

Culture	PGE_2 produced (ng/ml)			
	Control	1 h	2 h	8 h
Int-407 monolayers	237.1 ± 16.2	349.3 ± 84.7	180.6 ± 18.6	162.9 ± 124.0
3-D Int-407 cells	18,724.3 ± 1,590	16,985 ± 1,240.0	14,142.9 ± 2,280	16,772.0 ± 73.6

[a] Time course of PGE_2 levels before and after *Salmonella* infection of 3-D Int-407 cells and Int407 monolayers. Monolayers of Int-407 cells in 24-well plates or 3-D Int-407 cells cultured in 24-well plates were infected for 1 h with serovar Typhimurium χ3339 at an MOI of approximately 50:1. After 1 h, cultures were further incubated with gentamicin (10 μg/ml) for another 7 h. At the indicated times after infection, culture supernatants were collected and analyzed for PGE_2 by enzyme immunoassay.

Salmonella-induced gastroenteritis. Several studies have documented that the actual requirement for intestinal invasion for the induction of *Salmonella*-induced enteritis is not clear. That is to say, while it is generally assumed that *Salmonella* invasiveness is important in virulence, the actual requirement for intestinal invasion for the induction of enteritis is not clear. Indeed, in bovine intestinal infections, the vast majority of the inoculum remains in an extracellular niche (44, 45), and it has been shown elsewhere that extracellular bacteria can translocate effector proteins in the absence of invasion and that these effector proteins are required for enteritis (5). Studies have indicated that invasion is not sufficient to induce transepithelial signaling that leads to polymorphonuclear leukocyte migration associated with enteritis (32). Moreover, the secreted type III effector protein SipA is sufficient, in the absence of invasion, to induce a protein kinase C-dependent proinflammatory response in epithelial cells (29). These results bring into question the requirement for invasion in the induction of *Salmonella*-induced gastroenteritis. Accordingly, the lower levels of invasion observed for the 3-D Int-407 cells following *Salmonella* infection than for monolayers would appear to be in agreement with the above studies.

Although *Salmonella* adhered to and invaded the 3-D intestinal cells poorly, these cells did exhibit signs of *Salmonella*-induced damage at later postinfection time points. The question arises as to how *Salmonella* is able to induce damage in the host epithelium if it poorly adheres to and invades this tissue. In vitro studies have shown that the type III secretion system encoded on *Salmonella* pathogenicity island I is required for the translocation of proteins into host epithelial cells and the induction of fluid secretion and inflammatory responses (11, 12, 40). Given the inherent differences between the structural modifications of the surfaces of the 3-D intestinal epithelial cells and those for monolayers, it is possible that the secretion of type III effector proteins is induced in a different manner in the 3-D aggregates following *Salmonella* infection.

Both in vitro and in vivo studies have shown that interaction of wild-type virulent serovar Typhimurium with intestinal epithelium induces a number of morphological changes in the host epithelium important for subsequent bacterial invasion. These changes include cytoskeletal rearrangement with the formation of membrane ruffles upon the site of *Salmonella* contact, blunting and transient denuding and/or degeneration of microvilli from enterocytes, destruction of M cells, and the formation of pathological lesions (reviewed in reference 11). In this study, we show that 3-D Int-407 aggregates displayed minimal change in overall morphology following *Salmonella* infection compared to the extensive loss of integrity observed for Int-407 monolayers following the same time course of infection. Since the 3-D aggregates more closely resemble human intestinal epithelium, the difference in structural integrity following *Salmonella* infection of these tissues compared to monolayers is likely more reflective of an in vivo infection.

Induction of tissue damage in the form of apoptosis is a common response of host tissues to infection with bacterial pathogens. Indeed, several mediators produced in response to *Salmonella* infection, such as TNF-α, also have the potential to induce apoptosis of epithelial cells (25). Not surprisingly, *Salmonella* spp. have been shown previously to induce apoptosis following infection of several cell types, including cultured macrophages (4, 36) and a human colonic epithelial cell line (25). However, the onset of cell apoptosis in each of these cell types following *Salmonella* infection was much different, with a rapid onset of apoptosis (within 2 h) following infection of macrophages (4, 36) and a delay of up to 12 to 18 h following bacterial entry into colon epithelial cell lines (25). It is important to note that previous studies investigating *Salmonella*-induced apoptosis of epithelial cells have used different cell lines and/or different strains of *Salmonella* than those used in our studies. In our studies, the percent apoptosis in Int-407 cells grown as monolayers was significantly increased 90 min postinfection with *Salmonella* compared to uninfected controls. Specifically, we observed a rapid onset of apoptosis following *Salmonella* infection of Int-407 monolayers, with a 70 to 90% apoptotic index occurring 90 min after infection. However, there was no difference in apoptosis between infected and uninfected 3-D Int-407 tissue aggregates at the same time postinfection. These data are in agreement with the pathology of 3-D tissue aggregates relative to monolayers before and after infection with serovar Typhimurium. In addition, the results from adherence and invasion studies also support these observations, as *Salmonella* adherence to and invasion into 3-D Int-407 aggregates were significantly less than those observed for Int-407 monolayers. Considering that the vast majority of cases of *Salmonella*-induced gastroenteritis go unreported (less than 5% reported), it seems unlikely that, following ingestion of *Salmonella*, approximately 70% of human intestinal epithelial cells undergo apoptotic death. Thus, the lower levels of apoptosis observed following *Salmonella* infection of 3-D human intestinal aggregates would likely be more reflective of an in vivo infection.

Recent work with cultured epithelial cell lines has begun to elucidate the molecular mechanisms by which *Salmonella* induces inflammation (reviewed in reference 6). While the exact model by which *Salmonella* triggers diarrhea remains incompletely defined, results from both in vivo and in vitro studies suggest that, in response to *Salmonella* invasion, epithelial cells rapidly up-regulate the expression and secretion of an array of cytokines known to be important for the initiation of an acute inflammatory response, including TNF-α (24) and an array of proinflammatory mediators, like IL-8 (8, 31) and pathogen-elicited epithelial chemoattractant (33), that chemoattract neutrophils and mononuclear phagocytes to the site of infection. Thus, in the early stages following *Salmonella* invasion, epithelial cells produce mediators that have the potential to orchestrate the onset of the mucosal inflammatory response. Moreover, it is possible that the increased expression of the proinflammatory cytokines TNF-α and IL-6 by the Int-407 monolayers compared to the 3-D aggregates in response to *Salmonella* infection is, in part, responsible for the dramatic increase in damage to the monolayers compared to 3-D Int-407 tissue aggregates. Furthermore, the enhanced basal level of expression of TGF-β1 by the uninfected 3-D Int-407 cells compared to monolayers is relevant to the in vivo condition, in which the intestinal mucosa constitutively produces high levels of this cytokine (46).

We show in this work that Int-407 monolayers responded to infection with *Salmonella* by increasing the transcriptional expression of genes encoding the proinflammatory and immunomodulatory cytokines IL-1α, IL-1β, IL-6, and TNF-α, the last

of which has been shown previously to induce apoptosis in several cell types (1, 2, 19, 42). In contrast, 3-D Int-407 tissue aggregates infected with *Salmonella* increased expression of the anti-inflammatory cytokine IL-1Ra. These results suggest that the relatively undifferentiated Int-407 monolayers react differently to infection with *Salmonella* than do the 3-D Int-407 tissue aggregates. Although infection of 3-D Int-407 tissue aggregates with *Salmonella* stimulated increased transcription of these same cytokines, the magnitude of induction of expression was markedly less than with Int-407 monolayers.

In vitro and in vivo studies have reported that, following infection with *Salmonella*, increased prostaglandin synthesis by polymorphonuclear leukocytes (14–16) and epithelial cells (9) is important for the increased fluid secretion from intestinal epithelium. However, the role of prostaglandins in the development of *Salmonella*-induced diarrheal disease in humans has not been established. It has been suggested that, in addition to regulating gastrointestinal fluid secretion, epithelium-derived prostaglandins may limit the extent of mucosal injury following infection with invasive bacteria (35, 38). While it is unclear as to how prostaglandins may exert mucosa-protective events, they have been shown previously to down-regulate the production of several proinflammatory cytokines, such as IL-1 (26). The results from our studies are in agreement with a role for prostaglandins in mediating a protective response against *Salmonella*-induced damage to the epithelial mucosa. We have demonstrated that constitutive levels of PGE_2 synthesis in uninfected 3-D Int-407 cells were significantly higher than those observed for uninfected monolayer cultures.

To our knowledge, this report is the first to investigate the use of 3-D tissue aggregates cultured in the RWV as a model for microbial infectivity by a bacterial pathogen. It is anticipated that information obtained from these studies may bridge the gap between the inherent limitations of traditional tissue culture methodology and animal models which are currently used for investigation of *Salmonella* infectivity. Moreover, results from these studies suggest that the use of the RWV to generate 3-D aggregates from a variety of cell types may have wide applications in the modeling of infectious diseases.

ACKNOWLEDGMENTS

We thank Ed Benes for assistance with flow cytometry experiments, Erica Bell for assistance with cultivation and maintenance of tissue culture cells. Helena Pappas-LeBeau for histological staining, Brian Morrow for critical review of the manuscript, James Wilson for helpful discussions, Bruno Sainz for assistance with photographic imaging, and Theron Groves and the Microbiology Laboratory at the Johnson Space Center for technical support.

This work was supported, in part, by NASA-Ames grant NAG 2-1378 and by a generous grant from the W. M. William Keck Foundation of Los Angeles, Calif.

REFERENCES

1. **Abreu-Martin, M. T., A. Vidrich, D. H. Lynch, and S. R. Targan.** 1995. Divergent induction of apoptosis and IL-8 secretion in HT-29 cells in response to TNF-alpha and ligation of Fas antigen. J. Immunol. **155:**4147–4154.
2. **Browning, J. L., K. Miatkowski, I. Sizing, D. Griffiths, M. Zafari, C. D. Benjamin, W. Meier, and F. Mackay.** 1996. Signaling through the lymphotoxin beta receptor induces the death of some adenocarcinoma tumor lines. J. Exp. Med. **183:**867–878.
3. **Carson, F. L.** 1997. H&E regressive method, p. 96. *In* F. L. Carson (ed.), Histotechnology; a self-instructional text. ASCP Press, Chicago, Ill.
4. **Chen, L. M., K. Kaniga, and J. E. Galan.** 1996. *Salmonella* spp. are cytotoxic for cultured macrophages. Mol. Microbiol. **21:**1101–1115.
5. **Collazo, C. M., and J. E. Galan.** 1997. The invasion-associated type III system of *Salmonella typhimurium* directs the translocation of Sip proteins into host cells. Mol. Microbiol. **24:**747–756.
6. **Darwin, K. H., and V. L. Miller.** 1999. Molecular basis of the interaction of *Salmonella* with the intestinal mucosa. Clin. Microbiol. Rev. **12:**405–428.
7. **Devine, P. L.** 1992. A sensitive microplate assay for glycoproteins that utilizes an immunological digoxigenin-based detection system. BioTechniques **12:**160–162.
8. **Eckmann, L., M. F. Kagnoff, and J. Fierer.** 1993. Epithelial cells secrete the chemokine interleukin-8 in response to bacterial entry. Infect. Immun. **61:**4569–4574.
9. **Eckmann, L., W. F. Stenson, T. C. Savidge, D. C. Lowe, K. E. Barrett, J. Fierer, J. R. Smith, and M. F. Kagnoff.** 1997. Role of intestinal epithelial cells in the host secretory response to infection by invasive bacteria. Bacterial entry induces epithelial prostaglandin h synthase-2 expression and prostaglandin E2 and F2alpha production. J. Clin. Investig. **100:**296–309.
10. **Freshney, R. I.** 2000. Culture of animal cells: a manual of basic technique, 4th ed. Wiley-Liss, Inc., New York, N.Y.
11. **Galan, J. E., and J. B. Bliska.** 1996. Cross-talk between bacterial pathogens and their host cells. Annu. Rev. Cell Dev. Biol. **12:**221–255.
12. **Galyov, E. E., M. W. Wood, R. Rosqvist, P. B. Mullan, P. R. Watson, S. Hedges, and T. S. Wallis.** 1997. A secreted effector protein of *Salmonella dublin* is translocated into eukaryotic cells and mediates inflammation and fluid secretion in infected ilcal mucosa. Mol. Microbiol. **25:**903–912.
13. **Giannasca, P. J., K. T. Giannasca, A. M. Leichtner, and M. R. Neutra.** 1999. Human intestinal M cells display the sialyl Lewis A antigen. Infect. Immun. **67:**946–953.
14. **Giannella, R. A., S. B. Formal, G. J. Dammin, and H. Collins.** 1973. Pathogenesis of salmonellosis. Studies of fluid secretion, mucosal invasion, and morphologic reaction in the rabbit ileum. J. Clin. Investig. **52:**441–453.
15. **Giannella, R. A., R. E. Gots, A. N. Charney, W. B. Greenough III, and S. B. Formal.** 1975. Pathogenesis of *Salmonella*-mediated intestinal fluid secretion. Activation of adenylate cyclase and inhibition by indomethacin. Gastroenterology **69:**1238–1245.
16. **Giannella, R. A., W. R. Rout, and S. B. Formal.** 1977. Effect of indomethacin on intestinal water transport in *Salmonella*-infected rhesus monkeys. Infect. Immun. **17:**136– 139.
17. **Ginocchio, C.** 1995. The initial bacterial and host cell events of *Salmonella* infections. Clin. Microbiol. Updates **7:**1–7.
18. **Goodwin, T. J., W. F. Schroeder, D. A. Wolf, and M. P. Moyer.** 1993. Rotating-wall vessel coculture of small intestine as a prelude to tissue modeling: aspects of simulated microgravity. Proc. Soc. Exp. Biol. Med. **202:**181–192.
19. **Grell, M., G. Zimmermann, D. Hulser, K. Pfizenmaier, and P. Scheurich.** 1994. TNF receptors TR60 and TR80 can mediate apoptosis via induction of distinct signal pathways. J. Immunol. **153:**1963–1972.
20. **Gulig, P. A., and R. Curtiss.** 1987. Plasmid-associated virulence of *Salmonella typhimurium*. Infect. Immun. **55:**2891–2901.
21. **Hammond, T. G., and J. M. Hammond.** 2001. Optimized suspension culture: the rotating-wall vessel. Am. J. Physiol. Renal Physiol. **281:**F12–F25.
22. **Henle, G., and F. Deinhardt.** 1957. The establishment of strains of human cells in tissue culture. J. Immunol. **79:**54–59.
23. **Hook, E. W.** 1985. *Salmonella* species (including typhoid fever), p. 1258–1268. *In* R. G. Douglas, and G. L. Mandell (ed.), Principles and practice of infectious diseases. John Wiley & Sons, Inc., New York, N.Y.
24. **Jung, H. C., L. Eckmann, S. K. Yang, A. Panja, J. Fierer, E. Morzycka-Wroblewska, and M. F. Kagnoff.** 1995. A distinct array of proinflammatory cytokines is expressed in human colon epithelial cells in response to bacterial invasion. J. Clin. Investig. **95:**55–65.
25. **Kim, J. M., L. Eckmann, T. C. Savidge, D. C. Lower, T. W. Witthoft, and M. F. Kagnoff.** 1998. Apoptosis of human intestinal epithelial cells after bacterial invasion. J. Clin. Investig. **102:**1815–1823.
26. **Knudsen, P. J., C. A. Dinarello, and T. B. Strom.** 1986. Prostaglandins posttranscriptionally inhibit monocyte expression of interleukin 1 activity by increasing intracellular cyclic adenosine monophosphate. J. Immunol. **137:**3189–3194.
27. **Krakauer, T., J. Vilcek, and J. J. Oppenheim.** 1999. Proinflammatory cytokines: TNF and IL-1 families, chemokines, TGF-β, and others, p. 802–803. *In* W. E. Paul (ed.), Fundamental immunology. Lippincott-Raven Publishers, Philadelphia, Pa.
28. **Kruse, P. F., Jr., and M. K. Patterson, Jr.** 1973. Tissue culture—methods and applications. Academic Press, New York, N.Y.
29. **Lee, C. A., M. Silva, A. M. Siber, A. J. Kelly, E. Galyov, and B. A. McCormick.** 2000. A secreted *Salmonella* protein induces a proinflammatory response in epithelial cells, which promotes neutrophil migration. Proc. Natl. Acad. Sci. USA **97:**12283–12288.
30. **Lennox, E. S.** 1955. Transduction of linked genetic characters of the host by bacteriophage P1. Virology **1:**190–206.
31. **McCormick, B. A., S. P. Colgan, C. Delp-Archer, S. I. Miller, and J. L. Madara.** 1993. *Salmonella typhimurium* attachment to human intestinal ep-

ithelial monolayers: transcellular signalling to subepithelial neutrophils. J. Cell Biol. **123:**895–907.
32. **McCormick, B. A., S. I. Miller, D. Carnes, and J. L. Madara.** 1995. Transepithelial signaling to neutrophils by salmonellae: a novel virulence mechanism for gastroenteritis. Infect. Immun. **63:**2302–2309.
33. **McCormick, B. A., C. A. Parkos, S. P. Colgan, D. K. Carnes, and J. L. Madara.** 1998. Apical secretion of a pathogen-elicited epithelial chemoattractant activity in response to surface colonization of intestinal epithelia by *Salmonella typhimurium*. J. Immunol. **160:**455–466.
34. **Miller, V. L.** 1995. Tissue-culture invasion: fact or artcfact? Trends Microbiol. **3:**69–71.
35. **Mizuno, H., C. Sakamoto, K. Matsuda, K. Wada, T. Uchida, H. Noguchi, T. Akamatsu, and M. Kasuga.** 1997. Induction of cyclooxygenase 2 in gastric mucosal lesions and its inhibition by the specific antagonist delays healing in mice. Gastroenterology **112:**387–397.
36. **Monack, D. M., B. Raupach, A. E. Hromockyj, and S. Falkow.** 1996. *Salmonella typhimurium* invasion induces apoptosis in infected macrophages. Proc. Natl. Acad. Sci. USA **93:**9833–9838.
37. **Nickerson, C. A., and R. Curtiss III.** 1997. Role of sigma factor RpoS in initial stages of *Salmonella typhimurium* infection. Infect. Immun. **65:**1814–1823.
38. **Reuter, B. K., S. Asfaha, A. Buret, K. A. Sharkey, and J. L. Wallace.** 1996. Exacerbation of inflammation-associated colonic injury in rat through inhibition of cyclooxygenase-2. J. Clin. Investig. **98:**2076–2085.
39. **Rosenshine, I., S. Ruschkowski, V. Foubister, and B. B. Finlay.** 1994. *Salmonella typhimurium* invasion of epithelial cells: role of induced host cell tyrosine protein phosphorylation. Infect. Immun. **62:**4969–4974.
40. **Tsolis, R. M., L. G. Adams, T. A. Ficht, and A. J. Baumler.** 1999. Contribution of *Salmonella typhimurium* virulence factors to diarrheal disease in calves. Infect. Immun. **67:**4879–4885.
41. **Unsworth, B. R., and P. I. Lelkes.** 1998. Growing tissues in microgravity. Nat. Med. **4:**901–907.
42. **Van Antwerp, D. J., S. J. Martin, T. Kafri, D. R. Green, and I. M. Verma.** 1996. Suppression of TNF-alpha-induced apoptosis by NF-kappaB. Science **274:**787–789.
43. **Vanderburg, C. R., and E. D. Hay.** 1996. Exogenous E-cadherin expression in primary corneal fibroblasts leads to the formation of stratified epithelia. Acta Anat. **157:**87–104.
44. **Wallis, T. S., and E. E. Galyov.** 2000. Molecular basis of *Salmonella*-induced enteritis. Mol. Microbiol. **36:**997–1005.
45. **Watson, P., S. Paulin, A. Bland, P. Jones, and T. Wallis.** 1995. Characterization of intestinal invasion by *Salmonella typhimurium* and *Salmonella dublin* and effect of a mutation in the *invH* gene. Infect. Immun. **63:**2743–2754.
46. **Weiner, H. L.** 1994. Oral tolerance. Proc. Natl. Acad. Sci. USA **91:**10762–10765.
47. **Weinstein, D. L., B. L. O'Neill, D. M. Hone, and E. S. Metcalf.** 1998. Differential early interactions between *Salmonella enterica* serovar Typhi and two other pathogenic *Salmonella* serovars with intestinal epithelial cells. Infect. Immun. **66:**2310–2318.

Editor: A. D. O'Brien